Systematic and Applied Microbiology 37 (2014) 277–286

Contents lists available at ScienceDirect

Systematic and Applied Microbiology

journal homepage: www.elsevier.de/syapm

Physiology of *Geobacter metallireducens* under excess and limitation of electron donors. Part I. Batch cultivation with excess of carbon sources

Sviatlana Marozava[a], Wilfred F.M. Röling[b], Jana Seifert[c,d], Robert Küffner[e], Martin von Bergen[c,f,g], Rainer U. Meckenstock[a,*]

[a] *Institute of Groundwater Ecology, Helmholtz Zentrum München, Ingolstädter Landstraße 1, 85764 Neuherberg, Germany*
[b] *Department of Molecular Cell Physiology, Faculty of Earth and Life Sciences, VU University Amsterdam, De Boelelaan 1085, 1081 HV Amsterdam, The Netherlands*
[c] *Department Proteomics, Helmholtz Center for Environmental Research – UFZ, Permoserstraße 15, 04318 Leipzig, Germany*
[d] *Institute of Animal Nutrition, University of Hohenheim, Emil-Wolff-Str. 10, 70599 Stuttgart, Germany*
[e] *Teaching and Research Unit Bioinformatic, Institut für Informatik, Ludwig-Maximilians-Universität München, Amalienstr. 17, 80333 Munich, Germany*
[f] *Department Metabolomics, Helmholtz Center for Environmental Research – UFZ, Permoserstraße 15, 04318 Leipzig, Germany*
[g] *Department of Biotechnology, Chemistry and Environmental Engineering, Aalborg University, Sohngaardsholmsvej 49, DK-9000 Aalborg, Denmark*

ARTICLE INFO

Keywords:
Geobacter metallireducens
Carbon catabolite repression
Label-free proteomics

ABSTRACT

For microorganisms that play an important role in bioremediation, the adaptation to swift changes in the availability of various substrates is a key for survival. The iron-reducing bacterium *Geobacter metallireducens* was hypothesized to repress utilization of less preferred substrates in the presence of high concentrations of easily degradable compounds. In our experiments, acetate and ethanol were preferred over benzoate, but benzoate was co-consumed with toluene and butyrate. To reveal overall physiological changes caused by different single substrates and a mixture of acetate plus benzoate, a nano-liquid chromatography–tandem mass spectrometry-based proteomic approach (nano-LC–MS/MS) was performed using label-free quantification. Significant differential expression during growth on different substrates was observed for 155 out of 1477 proteins. The benzoyl-CoA pathway was found to be subjected to incomplete repression during exponential growth on acetate in the presence of benzoate and on butyrate as a single substrate. Peripheral pathways of toluene, ethanol, and butyrate degradation were highly expressed only during growth on the corresponding substrates. However, low expression of these pathways was detected in all other tested conditions. Therefore, *G. metallireducens* seems to lack strong carbon catabolite repression under high substrate concentrations, which might be advantageous for survival in habitats rich in fatty acids and aromatic hydrocarbons.

Introduction

In the environment, microorganisms are often exposed to mixtures of carbon sources, and accurate regulation of their uptake and metabolism is essential for survival of the fittest. Carbon catabolite repression (CCR) is an example of such a well-established global metabolic control of gene regulation in bacteria. It prioritizes the usage of one carbon source over another, when more than one is present. This happens via repression of genes responsible for degradation of less preferred carbon sources. As a result, bacteria exhibit high growth rates while utilizing the most energy efficient carbon substrates [55].

Surprisingly, it is unclear how gene regulation operates in the environment, especially in groundwater contaminated with hydrocarbons. Under such pollution regimes, microorganisms are exposed to anoxic conditions [10] and high concentrations of pollutants mixed with naturally occurring [21] or contaminant-associated organic acids [36]. Therefore, this study aimed to take a first step toward understanding metabolic regulation in strict anaerobic bacteria relevant for hydrocarbon-contaminated aquifers.

CCR has been studied extensively since the early 1940s when Jacques Monod discovered diauxic growth of *Bacillus subtilis*

* Corresponding author. Tel.: +49 89 3187 2560; fax: +49 89 3187 3361.
E-mail address: rainer.meckenstock@helmholtz-muenchen.de (R.U. Meckenstock).

http://dx.doi.org/10.1016/j.syapm.2014.02.004
0723-2020/

[19,37]. However, only a few studies have addressed CCR in anaerobic bacteria. Glucose has been shown to repress utilization of xylose and lactose in the strict anaerobe *Clostridium acetobutylicum* [20] and the thermophilic Gram-negative bacterium *Thermotoga neapolitana*, respectively [39,54]. Utilization of the aromatic compound benzoate can be repressed, co-utilized or preferred in facultative anaerobes. For example, in *Azoarcus* sp. strain CIB benzoate consumption is repressed by succinate, malate, and acetate [5], and in *Thauera aromatica* benzoate is simultaneously utilized together with succinate [51], while it is preferentially consumed over succinate in *Aromatoleum aromaticum* EbN1 [51].

To the best of our knowledge, there is a lack of information on CCR in strictly anaerobic aromatic compound-degrading microorganisms, such as *Geobacter metallireducens.* Iron-reducing *Geobacter* species are very abundant in Fe(III) rich environments contaminated with aromatic hydrocarbons [33]. *G. metallireducens* degrades many common petroleum-derived pollutants, including toluene, phenol, and *p*-cresol [32]. This bacterium is also capable of utilizing common fermentation products, such as acetate, butyrate, and ethanol [31].

The aim of the current study was to investigate whether *G. metallireducens* could perform preferential consumption of fermentation products (acetate, butyrate, and ethanol) over model aromatic compounds (toluene, benzoate) under batch culture conditions, and how the presence of sole carbon sources and a mixture of acetate plus benzoate influenced the expression of the corresponding pathways. The data obtained were used as a reference for a subsequent investigation concerning the physiology of *G. metallireducens* under carbon-limiting conditions and extremely low growth rates [34].

Materials and methods

Organism and cultivation media

G. metallireducens (strain GS-15/ATCC 53774/DSM 7210) was purchased from the Deutsche Sammlung von Mikroorganismen und Zellkulturen GmbH (DSMZ), Germany. Microorganisms were cultivated under anoxic conditions in a mineral medium (DSMZ Geobacter medium 579) with DSMZ trace element solution SL10 ($1\,mL\,L^{-1}$) and DSMZ 7 vitamins solution ($0.5\,mL\,L^{-1}$). Single substrates were added (acetate (5 mM), benzoate (1 mM), butyrate (20 mM), ethanol (20 mM), and toluene (1 mM)) and Fe(III) citrate (50 mM) was used as the electron acceptor. For diauxic experiments, the following concentrations were used: 2 mM acetate plus 0.6 mM benzoate, 2.5 mM acetate plus 0.5 mM toluene, 0.3 mM benzoate plus 0.5 mM toluene, 2 mM acetate plus 3 mM butyrate, 2.5 mM acetate plus 2 mM ethanol, 4 mM butyrate plus 2 mM ethanol, 4.5 mM butyrate plus 0.4 mM benzoate, 1 mM ethanol plus 0.5 mM benzoate together with 50 mM Fe(III) citrate (Table 1). All experiments were performed in triplicates, and 80 mL of medium were dispensed into sterile 100 mL bottles. The bottles were flushed with a mixture of N_2 and CO_2 (80%: 20%) and sealed with butyl rubber stoppers. When toluene was used as a substrate, the bottles were sealed with Viton® rubber stoppers. All incubations were performed at 30 °C in the dark. Growth rate estimations were based on the concentration of Fe^{2+} produced. The inoculation of the single substrate experiments was carried out with cells pre-grown on the same substrate used for the respective experiments. The substrates used for precultivation of inoculum of the dual substrate experiments are indicated in Table 1. Preliminary experiments showed that the carbon source used to cultivate the inoculum did not influence the substrate consumption profile in the experiments with mixed substrates (data not shown). Moreover, in order to determine the influence of acetate on expression of the benzoyl-CoA-degrading pathway and eliminate a possible pre-history in the expression of any pathway, cells were pre-grown on acetate for at least three generations and then inoculated into the medium with acetate plus benzoate.

Chemical analysis

Fe^{2+} was measured using the ferrozine assay according to Braunschweig et al. [8].

Acetate and butyrate were measured by HPLC (Shimadzu, Japan) on an Aminex HPX87H column (Bio-Rad) with 0.5 mM H_2SO_4 as a mobile phase (column temperature: 50 °C, flow rate: $0.5\,mL\,min^{-1}$, UV detection at 220 nm). A total of 0.5 mL of sample was treated with 55 μL of 35% perchloric acid, incubated for 10 min on ice, and then 27 μL of 7 M KOH was added before it was stored at −20 °C. Before the measurements, the samples were thawed at room temperature, centrifuged at $17{,}900 \times g$ for 2 min and the supernatant was filtered through Millipore filters (Millex-HV, 0.45 μm). Samples for benzoate measurements were treated with 1 M NaOH (1:10 dilution), incubated on ice for 10 min, and stored at 4 °C overnight. Before the measurements, 80% ethanol was added in a 1:1 ratio and samples were centrifuged for 2 min at $20{,}800 \times g$. Benzoate was analyzed on a PFP Kinetex column (Phenomenex Inc., USA). Elution took place isocratically with 1% acetic acid in Millipore water (solvent A) and 1% acetic acid in methanol (solvent B) (50:50, v:v) at a flow rate of $0.7\,mL\,min^{-1}$ (UV detection at 236 nm). Toluene was measured by GC–MS, as described elsewhere [4]. Ethanol was measured by a GC-FID (Hewlett Packard 5890 Series II) equipped with a 30 m VOCOL column, 0.25 mm inner diameter (Supelco, Bellefonte, Pennsylvania, USA), a film thickness of 1.5 μm and operated with nitrogen as a carrier gas at $1.6\,mL\,min^{-1}$. Sample application was performed by automated headspace injection of 1 mL from 10 mL headspace vials using a CombiPal Autosampler (CTC Analytics), and an injector temperature of 200 °C. The temperature program started at 80 °C (0.3 min), ramp $30\,°C\,min^{-1}$ to 160 °C (3.67 min), and $60\,°C\,min^{-1}$ to 200 °C (10.33 min).

Proteomic analyses

Cells were harvested during early exponential batch growth, except for one biological replicate on acetate plus benzoate where the proteome was also investigated in the late exponential phase. Cells were harvested by centrifugation at $3{,}400 \times g$ for 20 min, at 4 °C; washed once with 1× phosphate buffered saline (PBS) consisting of (per liter) NaCl (8 g), KCl (0.2 g), KH_2PO_4 (0.24 g), and Na_2HPO_4 (1.44 g). Washed cells were centrifuged again at $15{,}300\,x \times g$ for 1 min at 4 °C. Proteins for proteomic analyses were extracted by lysis buffer (2% sodium dodecyl sulfate (SDS), 20 mM Tris/HCl, pH 7.5) with sonication. The cell pellet was dissolved in SDS–lysis buffer and shaken for 5 min at 60 °C at 1400 rpm in Eppendorf thermomixer comfort. Then, 20 mM Tris/HCL pH 7.5 buffer with $1\,\mu L\,mL^{-1}$ benzonase (Novagen) (added directly before use), $0.1\,mg\,mL^{-1}$ $MgCl_2$, and 1 mM phenylmethylsulfonyl fluoride (PMSF) were added. Sonication was applied twice for 1 min (0.3 s per pulse, 30% duty) (ultrasonic processor UP50H, Hielscher Ultrasonics, Germany) with sample cooling on ice between the rounds.

Protein concentration was determined using the Bradford protein assay (Bio-Rad) with bovine serum albumin as the standard [7].

For one-dimensional gel electrophoresis, 50 μg of protein extract were precipitated with a five-fold volume of ice-cold acetone and resuspended in a loading buffer [29]. Acrylamide gels (12%) were stained with colloidal Coomassie Brilliant Blue G-250 (Roth, Kassel, Germany). The lanes of separated proteins were cut into five slices and digested over night at 37 °C with trypsin [25].

Table 1
Batch experiments using dual substrate mixtures with indication of the type of consumption.[a]

Pre-grown substrate	Co-substrate	Type of consumption	Lag phase (h)
Acetate (2.5 mM)	Toluene (0.5 mM)	Preferential	13
Acetate (2 mM)	Benzoate (0.6 mM)	Preferential	None
Benzoate (0.3 mM)	Toluene (0.5 mM)	Simultaneous	None
Butyrate (3 mM)	**Acetate** (2 mM)	Preferential	None
Ethanol (2 mM)	Acetate (2.5 mM)	Preferential	None
Butyrate (4 mM)	Ethanol (2 mM)	Simultaneous	None
Butyrate (4.5 mM)	Benzoate (0.4 mM)	Simultaneous	None
Benzoate (0.5 mM)	**Ethanol** (1 mM)	Preferential	36

[a] Substrates in bold are the preferred substrates.

Protein identification

Biological triplicates were investigated per condition and each biological sample was analyzed in two technical replicates. Peptides were analyzed by UPLC-LTQ Orbitrap-MS/MS as described in Bastida et al. [6]. The peptides were eluted over 50 min with a gradient of solvent B (8–40% acetonitrile). Continuous scanning of eluted peptide ions was carried out between a m/z range of 300–1600, automatically switching to MS/MS CID mode when ions exceeded an intensity of 3000. Identification was performed with MaxQuant (v. 1.2.2.5) [11] and its built-in database search algorithm Andromeda [12] using annotated protein sequences of *G. metallireducens* GS-15 (Uniprot, May 2011). Five gel slices of a single gel band were defined as one experiment for LFQ calculations. Settings were the following: peptide modifications of methionine oxidation as variable and cysteine carbamidomethylation as fixed. Further settings were: first search ppm of 20, main search ppm of 6, maximum number of modifications per peptide 5, maximum missed cleavages 2 and a maximum charge for the peptide of 6. Parameters for identification were a minimum peptide length of five amino acids, a false peptide discovery rate of 1%, proteins and level of modification sites of 1%. A minimum of one unique peptide was required for protein identification. As has been mentioned elsewhere [15], some proteins only have one tryptic peptide that can be detected by mass spectrometry (MS). Apart from unmodified peptides, only peptides with oxidized methionine and carbamidomethylized cysteine were used for quantification. Only unique or razor peptides were chosen for use in quantification. Miscellaneous settings switched on were: re-quantify, keep low scoring versions of identified peptides, match between runs (time window of 2 min), label-free quantification and second peptides. Furthermore, label-free quantification was performed on protein intensities that were the summary of all peptide intensities per protein, where peptide intensities were the peak areas of the respective masses in MS.

Statistical analysis

Normalization

After log-transformation, all individual batch cultures exhibited approximately normal intensity distributions. Deviations of distributions between replicate substrate conditions were mostly due to differences in the mean or variance. Protein intensity was normalized by matching mean $\bar{x}_j$ and standard deviation σ_j for each batch j by transforming measurements for each $x'_{i,j}$:

$$x'_{i,j} = \frac{(x_{i,j} - \bar{x}_j)\sigma}{\sigma_j} + \bar{x} \quad (1)$$

where $\bar{x}$ and σ correspond to the mean and standard deviation across all proteins i and substrate conditions j, respectively.

Determination and clustering of differentially expressed proteins

After normalization, a one-way analysis of variance (ANOVA) was applied for each protein in order to determine significant differences in expression between the six groups (=growth conditions) of three biological replicates each. Subsequently, conditions where proteins exhibited significant differential expression were identified via pairwise t-tests. Both statistical tests quantify the significance of differential expression events via p-values that, in the case of large-scale datasets, need to be corrected for multiple testing to distinguish true discoveries from false random positive events. The p-values from ANOVA and the t-test were uniformly corrected by transforming them into respective false discovery rates (FDRs, i.e. the percentage of proteins with significant expression by chance) based on random permutations of the protein expression data. Each protein-specific expression profile vector was randomized a hundred times and ANOVA, as well as the t-test, were applied to the 100 randomized datasets, as described above. For each p-value derived from the measured data, 100 p-values were derived from the permuted data. Then, a given p-value derived from measured data was transformed via FDR = (100 × number of false positives)/(number of permutations × number of true positives), where true and false positives referred to the number of p-values computed from measured and permuted data, respectively, that were less than or equal to the given p-value. This approach to FDR calculation was adapted from significance analysis of microarrays [52] and was described in detail in [24]. Subsequently, a FDR threshold of 5% was applied in order to identify differentially expressed proteins and corresponding pairs of conditions. Six growth conditions resulted in 15 pairwise t-tests for each protein.

Correspondence analysis

Correspondence analysis was conducted in order to visualize similarities between the conditions. A two dimensional plot (drawn by the software PAST [22]) depicted differentially expressed proteins as identified by ANOVA for each of the six conditions. The visualization measured the similarities between all data points based on Eigen-values of Chi-squared distances [22].

Hypergeometric test

Pathways enriched in differentially expressed proteins were identified by the hypergeometric test. Enrichment can be quantified via p-values based on the assumption of hypergeometric distribution as adapted from GO-analysis strategies [3,16]. More specifically, given a pathway π and a pair of growth conditions a and b, the hypergeometric test estimates the significance of observing among the K_π pathway proteins k_π or more proteins that are significantly up-regulated in condition a compared to condition b. For the purpose of representation, the p-values derived from the hypergeometric distribution were transformed into z-scores via the inverse cumulative distribution function.

Hierarchical regulation analysis of the TCA cycle

Hierarchical regulation analysis determines to what extent changes in flux through an enzyme, due to an environmental perturbation (in this case, growth on different substrates), are explained by changes in enzyme concentration (hierarchical regulation; quantified by the so-called hierarchical regulation coefficient ρ_h) and by changes in the interaction of the particular enzyme with its substrate (products, effectors) (metabolic regulation; quantified by the metabolic regulation coefficient ρ_m) [43,50]. For detailed mathematical derivation of the framework of hierarchical regulation analysis, including Eqs. (2) and (3) below, we referred to ter Kuilr and Westerhoff [50].

The hierarchical regulation coefficient ρ_h corresponds to the relative change in the concentration of an enzyme e_i upon a perturbation divided by the relative change of flux J due to the same enzyme e_i, according to Eq. (2) [50]:

$$\rho_h = \frac{\Delta \ln e_i}{\Delta \ln J} \quad (2)$$

In Eq. (2), delta (Δ) indicates the difference between two states. ρ_h is easily determined as the slope of a double logarithmic plot of the concentration of enzyme e_i against the corresponding flux J through the same enzyme for a number of conditions (in this case, growth on different substrates) [50]. Based on the summation theorem derived in ter Kuile and Westerhoff [50] and shown in Eq. (3), once the hierarchical regulation coefficient has been obtained, the metabolic regulation coefficient can be calculated easily:

$$\rho_h + \rho_m = 1 \quad (3)$$

Thus, a major advantage of hierarchical regulation analysis is that it allows this regulation to be differentiated from metabolic regulation without requiring any information on intracellular metabolite concentrations and kinetic parameters.

In the current study, the enzyme concentration e_i was represented by normalized averaged protein abundances (Supplementary Table S5) measured at maximum specific growth rates (μ_{max}, h^{-1}). The flux J due to the enzyme was calculated based on the turnover of the intermediate metabolite acetyl-CoA (the first central intermediate in the degradation of all five carbon sources studied here, and the compound entering the TCA cycle) as:

$$J = \frac{\mu_{max}}{Y} \quad (4)$$

where J is the flux [mmol acetyl-CoA $cell^{-1}$ h^{-1}], and Y is the yield of acetyl-CoA [cells $mmol^{-1}$ acetyl-CoA consumed]. μ_{max} was determined during the exponential phase. Y was measured in the stationary phase; however, the biomass was primarily formed during the exponential phase, thus allowing flux J to be derived from μ_{max} and Y according to Eq. (4). Y is expressed as cells L^{-1} in the stationary phase divided by mmol L^{-1} acetyl-CoA equivalents consumed in the same phase. Calculations of amounts of acetyl-CoA equivalents consumed were based on the amount of Fe^{2+} produced in the stationary phase, the stoichiometric equations for butyrate, acetate, ethanol, benzoate and toluene degradation coupled to Fe^{2+} production (Eqs. (5)–(9)), and the stoichiometry of substrate degradation to acetyl-CoA on the basis of known metabolic pathways (1 mole each of butyrate, acetate, ethanol, benzoate and toluene are converted into 2, 1, 1, 3, and 3 mole of acetyl-CoA, respectively.).

$$\text{Butyrate}: C_4H_7O_2^- + 20Fe^{3+} + 10H_2O \rightarrow 20Fe^{2+} + 4HCO_3^- + 23H^+ \quad (5)$$

$$\text{Acetate}: C_2H_3O_2^- + 8Fe^{3+} + 4H_2O \rightarrow 8Fe^{2+} + 2HCO_3^- + 9H^+ \quad (6)$$

$$\text{Ethanol}: C_2H_6O + 12Fe^{3+} + 5H_2O \rightarrow 12Fe^{2+} + 2HCO_3^- + 14H^+ \quad (7)$$

$$\text{Benzoate}: C_7H_5O_2^- + 30Fe^{3+} + 19H_2O \rightarrow 30Fe^{2+} + 7HCO_3^- + 36H^+ \quad (8)$$

$$\text{Toluene}: C_7H_8 + 36Fe^{3+} + 21H_2O \rightarrow 36Fe^{2+} + 7HCO_3^- + 43H^+ \quad (9)$$

It is assumed that nearly all substrate enters the TCA cycle, as experimentally observed for acetate, and 90% is degraded [49].

ρ_h values were obtained using Kaleidograph software. Values close to 1 indicated the importance of hierarchical regulation, while ρ_h close to zero indicated the importance of metabolic regulation of flux changes due to an enzyme. Moreover, hierarchical coefficients with negative values indicated an antagonistic effect between the changes in the enzyme concentration and changes in the flux due to an enzyme (with a flux increase the enzyme concentration decreases) [43].

Results

Utilization of substrate mixtures

G. metallireducens was cultivated on various combinations of two substrates in order to determine the utilization patterns of substrate mixtures (Table 1).

During preferential substrate utilization in a mixture, the ratio of the consumption rate of the preferred substrate over that of the repressed one was assumed to be higher than the ratio of specific consumption rates exhibited by *G. metallireducens* on the respective single substrates (see supplementary material). In the mixture, the ratio of the consumption rates of acetate over that of toluene or benzoate (587.5 and 17.2, respectively) was higher than the ratio of their respective specific consumption rates when used as sole substrates (20 and 4.4, respectively) (Fig. 1A and B, Supplementary Table S2). These results supported the observed inhibition of benzoate and toluene utilization in the presence of acetate (Fig. 1A and B). Acetate inhibited consumption of benzoate to a lesser extent than that of toluene, and once acetate was depleted, benzoate utilization started immediately (Fig. 1A). In contrast, there was a lag phase of thirteen hours between the depletion of acetate and the start of toluene consumption (Fig. 1B). In a mixture of benzoate and toluene, the two substrates were consumed simultaneously (Fig. 1C, Supplementary Table S2).

Among the other substrate mixtures tested, ethanol had a distinct repressing effect on acetate and benzoate consumption, whereas it was co-metabolized with butyrate (Supplementary Fig. S1B, S1D, and S1C). Additionally, butyrate and benzoate were consumed simultaneously (Supplementary Fig. S1E).

Differential analysis of proteins expressed on different substrates by G. metallireducens

LC–MS/MS analysis of proteomes of cells incubated on five individual carbon sources (acetate, benzoate, butyrate, ethanol, and toluene) and a mixture of two substrates (acetate plus benzoate) detected a total of 1477 proteins out of 3519 predicted for *G. metallireducens*, with appropriate representation of cytoplasmic and membrane proteins [58] (Supplementary Fig. S2).

Out of all proteins detected, 155 were differentially expressed (false discovery rate (FDR) <5%; Supplementary Table S3). Correspondence analysis of their relative abundances revealed a clear

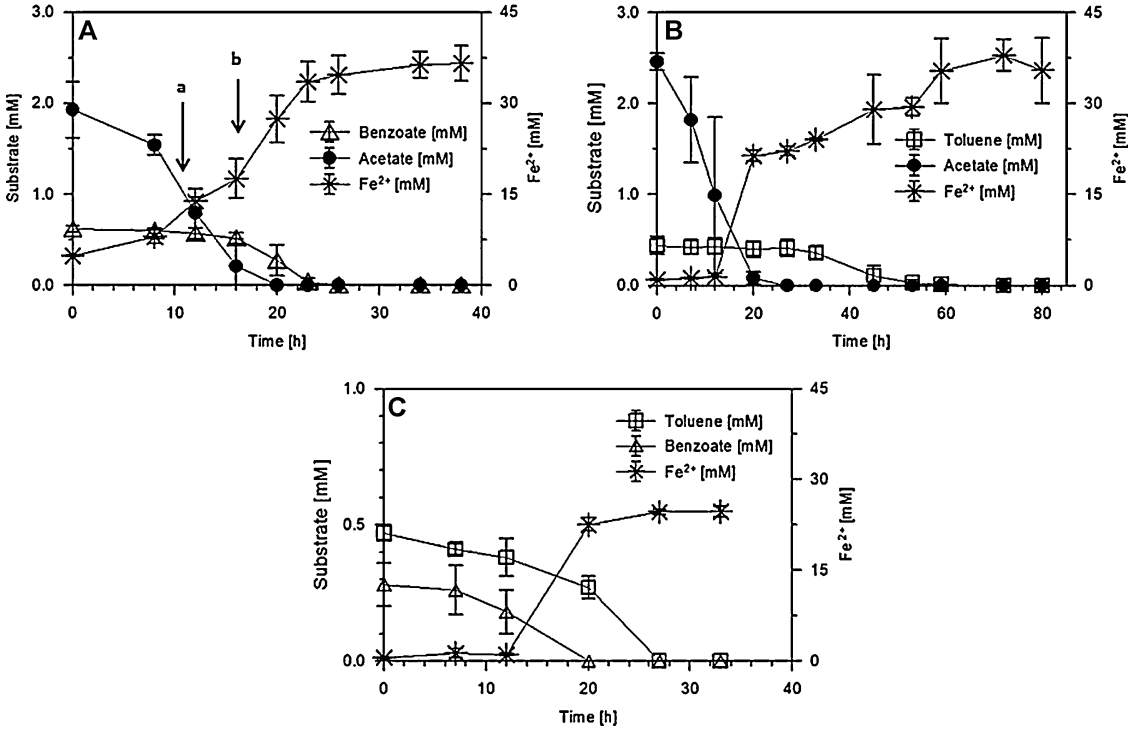

Fig. 1. Substrate consumption by *G. metallireducens* in batch cultures with acetate plus benzoate (A), toluene plus acetate (B), and toluene plus benzoate (C). Error bars indicate the standard deviations of three replicates. Arrows represent the sampling time for proteomic analysis: a, early exponential phase; b, late exponential phase.

separation of the five different single substrate growth conditions (Fig. 2). For the mixed substrate growth condition (acetate plus benzoate), the proteomes of cells in the early exponential phase closely resembled those observed during growth on acetate or were between proteomes of cells grown with acetate and benzoate, whereas the proteomes of cells in the late exponential phase showed high similarity to the proteomes during growth on benzoate only (Fig. 2).

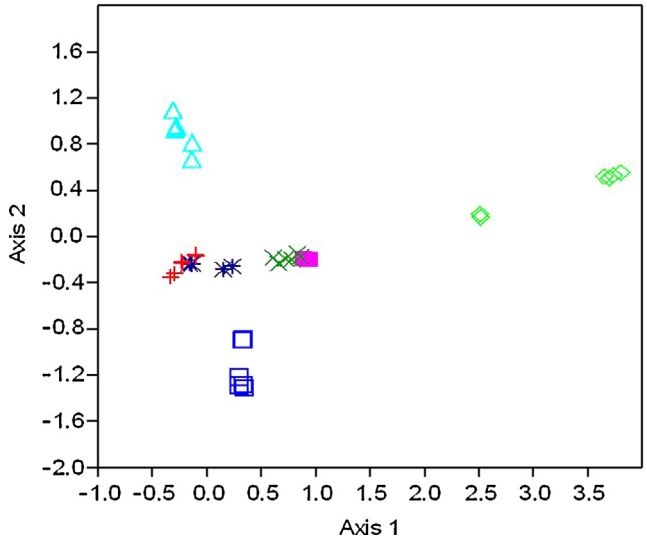

Fig. 2. Correspondence analysis on the basis of the abundances of 155 differentially expressed proteins for the various substrates on which *G. metallireducens* was grown. The two axes with the highest Eigen-values represent 46% of the variance. Symbols depict the different growth substrates: ◇, ethanol; △, toluene; ■, acetate plus benzoate (early exponential phase, acetate consumption); +, acetate plus benzoate (late exponential phase, all acetate consumed); ✱, benzoate; □, butyrate; ×, acetate. Normalized data used for correspondence analysis can be found in Supplementary Table S5.

All differentially expressed proteins were partitioned based on the chromosomal location of their corresponding genes, thus revealing distinct genomic regions (located at gene coordinates 1723k–1742k, 1843k–1942k, and 2017k–2423k) coding for toluene, butyrate or benzoate-degrading proteins, respectively (Fig. 3 and Supplementary Table S4). The majority of highly abundant proteins in the clusters were involved in the degradation of the corresponding carbon source(s) (Fig. 3 and Supplementary Table S4). However, most of these proteins were also detected at low levels during exponential growth on the other substrates (Supplementary Table S5). The remaining 56 differentially expressed proteins that were not associated with the above genomic regions were compiled into a fourth cluster named 'other'.

Toluene cluster

All thirteen proteins assigned to this cluster obtained highest abundances during growth on toluene. The cluster contained enzymes involved in β-oxidation of benzylsuccinate to benzoyl-CoA (BbsABCD and BbsEFGH) [9], and other products of the genomic toluene degradation island [9], such as electron transfer flavoproteins (Gmet_1525-Gmet_1527) and a protein with ATPase activity (Gmet_1537), which is 82.5% similar to chaperone-like ATPase (BssE) of *A. aromaticum* and might be required for functioning of benzylsuccinate synthase [27].

Benzoate cluster

Most of the 35 proteins assigned to this cluster were relatively highly abundant during exponential growth on benzoate, toluene, and butyrate, in comparison to acetate and ethanol (Fig. 3, Supplementary Table S4). Proteins with increased abundances during the early exponential growth on the mixture of acetate plus benzoate were related to benzoyl-CoA degradation (e.g. Gmet_2151-2153, Gmet_2074). During the late exponential phase, besides benzoyl-CoA degradation (e.g., Gmet_2151-2153), fatty acids-degrading

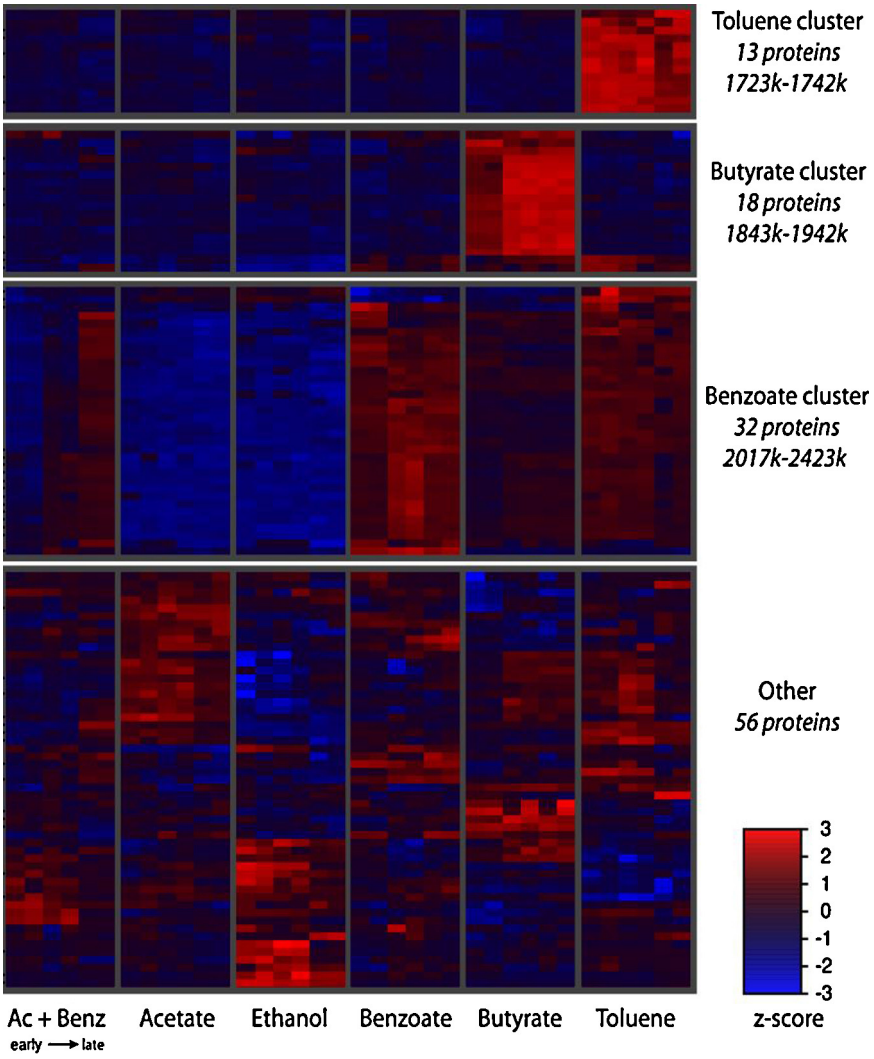

Fig. 3. Heat map representing the clustering of differentially expressed proteins on a mixture of acetate plus benzoate and five single substrates (acetate, benzoate, butyrate, ethanol, and toluene), as indicated below the map. The gene coordinates are indicated on the right hand side of the figure. Hierarchical cluster analysis was applied to each of the four groups separately. Protein expression is displayed in the heat map as *z*-scores (i.e. calculated based on the protein's mean and standard deviation) in the range between 3 (up-regulated, red) and −3 (down-regulated, blue). Whether the replicates were taken from early or late exponential phase on a mixture of acetate plus benzoate (Ac + Benz) is indicated below the condition name. (For interpretation of the references to color in this figure legend, the reader is referred to the web version of the article.)

(e.g. Gmet_2075, Gmet_2058-2059) and TCA cycle-related proteins (Gmet_2068-2069) were also enhanced (Supplementary Table S4). Succinyl:benzoate coenzyme A transferase (Gmet_2054) [40] was detected at significantly higher abundance only on benzoate compared to all other conditions, including the mixture of acetate and benzoate (Supplementary Table S4).

Butyrate cluster

Most of the butyrate-degrading proteins were abundant only with butyrate as a substrate (Fig. 3).

Protein cluster 'other'

This cluster contained proteins related to various functions (Supplementary Table S4), including enzymes related to ethanol degradation and the TCA cycle. The putative ethanol dehydrogenase (Gmet_1046) and aldehyde:ferredoxin oxidoreductase (Gmet_1045), which have high similarities to proteins putatively involved in ethanol degradation in *Pelobacter carbinolicus* [2], had the highest abundances on ethanol. Butyrate induced expression of two proteins from the TCA cycle, citrate synthase (Gmet_1124) and succinyl:acetate coenzyme A transferase (Gmet_1125), and they have also been suggested to be involved in propanoate utilization [1].

Differential analysis of catabolic pathways

A hypergeometric test revealed that single substrate growth conditions were characterized by differential expression of several peripheral degradation pathways (Fig. 4). For example, toluene induced significantly higher expression of the toluene-, benzoate-, and phenol-degrading pathways compared to acetate plus benzoate, acetate, and ethanol (Fig. 4E). Butyrate led to a significant increase not only in enzyme levels of the butyrate-degrading pathway but also in enzyme levels of the benzoate and propanoate pathways, compared to acetate plus benzoate, acetate, and ethanol (Fig. 4C).

Hierarchical regulation analysis of the TCA cycle

Hierarchical regulation analysis [50] was employed in order to quantify to what degree changes in the flux due to the enzymes of the TCA cycle, in response to growth on different substrates, were

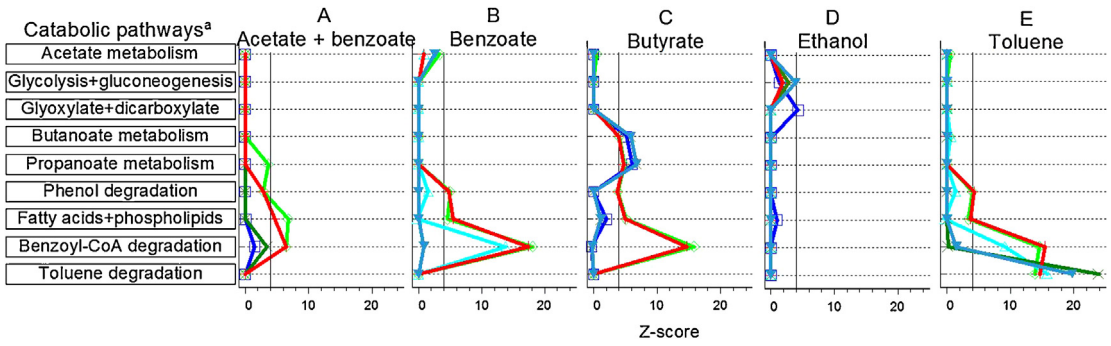

Fig. 4. Catabolic pathways expressed during growth on various substrates and representation of pairwise comparisons between the various growth conditions based on the metabolic pathways expressed. The *x*-axis represents the extent of relative expression of the catabolic pathways listed on the *y*-axis during the growth condition designated in the graph title (A–E) relative to another growth condition presented by the respective curve: , acetate plus benzoate; , acetate; , benzoate; , butyrate; , toluene; and , ethanol. Pathways with *z*-scores >4 (indicated by a vertical solid line) were considered to be significantly more abundant on one condition (A–E) relative to another (colored symbols). For example, in panel A, the benzoyl-CoA pathway (depicted on the *y*-axis) has *z*-score values >4, which indicates that the expression of this pathway is significantly higher on acetate plus benzoate (panel title A) compared to acetate (red line). [a]Proteins taken for hypergeometric analysis were assigned to the respective pathway via the internet search tool DAVID [14]. (For interpretation of the references to color in this figure legend, the reader is referred to the web version of the article.)

regulated by hierarchical changes in the expression levels of the TCA enzymes, as well as by changes in the interaction between metabolites and the TCA enzymes.

Most of the calculated hierarchical coefficients (ρ_h) for enzymes of the TCA cycle were close to zero and/or had negative values (Table 2), revealing a dominant role of metabolic regulation [43]. Thus, the hierarchical analysis suggested that changes in the flux through the TCA enzymes as a result of growth on different substrates did not require substantial changes in the expression of these enzymes, but were due to changes in metabolite concentrations and their interaction with enzymes.

Discussion

Is the benzoyl-CoA pathway repressed by aliphatic acids and alcohols in G. metallireducens?

The current study revealed that *G. metallireducens* did not utilize aromatic hydrocarbons in the presence of high concentrations of easily degradable substrates, such as acetate and ethanol. Similar observations have been made for other environmentally relevant microorganisms, such as the aerobic bacteria *Acinetobacter baylyi* [59], *Pseudomonas putida* [38] and *Pseudomonas stutzeri* A1501 [30], and the facultative anaerobe *Azoarcus* sp. strain CIB [5]. Preferential utilization of ethanol has been reported for BTEX degraders in aerobic and anaerobic microcosm experiments [13,44]. Although preferential utilization of benzoate over acetate or succinate has been reported [35,51], the repression of aromatic compound degradation by acetate and ethanol seems to prevail in a wide range of microorganisms, including *G. metallireducens*.

It is commonly assumed that the benzoyl-CoA pathway is repressed when *Geobacter* species are grown on acetate as the sole source of carbon [9,45,53,56]. The current study showed that during exponential growth in batch culture on acetate in the presence of benzoate the repression of the benzoyl-CoA pathway seemed to be less pronounced. This led to the observed readiness of the cells to degrade benzoate as soon as the repressor (acetate) was consumed (Fig. 1A). The significant expression of the benzoyl-CoA pathway in the presence of acetate suggested that benzoate entered the cell and induced expression of the pathway. To prove this hypothesis, increased expression of benzoate transporters needs to be detected during growth on acetate plus benzoate. However, the annotation of benzoate transporters for *G. metallireducens* has not been confirmed to date [1,9,23]. Among the putative transporters of aromatic hydrocarbons (Gmet_1534-Gmet_1537) [1], only Gmet_1535 was found to be expressed in all biological replicates on acetate plus benzoate (Supplementary Table S5). However, this protein is probably associated with toluene consumption as it was significantly more abundant only on toluene compared to all other conditions (Supplementary Table S4). Moreover, constitutive expression of benzoate transporters might be enough to induce the benzoyl-CoA degrading pathway.

Another important finding was the absence of significant expression of benzoyl-CoA ligase (Gmet_2143) during growth on benzoate. Instead, an alternative protein for the first step of benzoate degradation, succinyl:benzoate coenzyme A transferase (Gmet_2054) [40], was significantly more abundant on benzoate compared to all other conditions. The average abundance of this protein was fifty-seven times higher than that of benzoyl-CoA ligase on benzoate (Supplementary Table S5). Although the transcripts of the genes encoding both enzymes were found to be up-regulated on benzoate compared to acetate in the study of Butler et al. [9], our proteomic approach suggested that the transfer of CoA was preferred over ligation to benzoate as it is less energy demanding [40]. Among the tested growth conditions, the abundance of this protein was the highest on benzoate and on acetate plus benzoate during the late exponential phase in batch culture. Therefore, although the benzoyl-CoA pathway was found to be under weak carbon catabolite control in *G. metallireducens*, the significant expression of the protein responsible for the first step of benzoate degradation depended only on the presence of the respective substrate.

Expression of catabolic pathways in G. metallireducens grown on single substrates at high concentrations in batch culture

As expected, under conditions of carbon excess, enzymes conducting the first steps in substrate degradation were highly abundant in the presence of the corresponding substrates. However, enzymes catalyzing downstream reactions of substrates degradation were frequently found to be present during growth on other substrates, for example, benzoyl-CoA-degrading enzymes were detected not only on aromatic compounds but also on butyrate, acetate, and ethanol. Detection of proteins carrying out downstream reactions of aromatic compound degradation can be explained by weak carbon catabolite control of these proteins.

Table 2
Hierarchical regulation coefficients ρ_h for enzymes of the TCA cycle; ρ_h can take any value between −1 and 1. Standard errors were calculated between six growth conditions.

Gene name	Enzyme	ρ_h	Standard error
Gmet_2689	Citrate synthase	0.005	0.240
Gmet_2763	Aconitase	−0.086	0.093
Gmet_1016	Aconitase	−0.003	0.055
Gmet_1912	Aconitate hydratase 2	−0.044	0.144
Gmet_1359	Isocitrate dehydrogenase [NADP]	−0.157	0.199
Gmet_2769	2-oxoglutarate dehydrogenase E1 component	−0.142	0.157
Gmet_1362	2-oxoglutarate ferredoxin oxidoreductase, alpha subunit	0.113	0.318
Gmet_1363	2-oxoglutarate ferredoxin oxidoreductase, beta subunit	0.216	0.202
Gmet_1364	2-oxoglutarate ferredoxin oxidoreductase, gamma subunit	−0.337	0.209
Gmet_2068	Succinyl-CoA ligase [ADP-forming] subunit alpha	−0.631	1.127
Gmet_0730	Succinyl-CoA ligase [ADP-forming] subunit alpha	−0.019	0.152
Gmet_0729	Succinyl-CoA ligase [ADP-forming] subunit beta 1	−0.090	0.109
Gmet_2397	Succinate dehydrogenase subunit C	−0.465	0.221
Gmet_2396	Succinate dehydrogenase subunit A	−0.401	0.168
Gmet_2395	Succinate dehydrogenase subunit B	−0.066	0.207
Gmet_2570	Fumarase	0.037	0.058
Gmet_1360	Malate dehydrogenase	0.305	0.265

The coordinated expression of the peripheral catabolic proteins described here can be partially explained by the co-localization of the respective genes on the genome (Fig. 3) [42]. Genes coding for toluene, butyrate, and benzoyl-CoA-degrading pathways occupy distinct sections on the chromosome. In addition to expected co-expression of aromatic-degrading pathways on toluene, the current study revealed unexpected co-expression of the benzoyl-CoA and butyrate-degrading pathways on butyrate (Figs. 3 and 4). Such co-expression was not observed on benzoate. This might suggest that butyrate-derived metabolic intermediates can also participate in the induction of the benzoyl-CoA-degrading pathway leading to the simultaneous consumption of benzoate and butyrate.

Co-metabolism of aromatic compounds is widespread among microorganisms [18]. For example, several xenobiotic-degrading pathways were found to be co-expressed in *P. putida* CB55 [57], *Mycobacterium aromativorans* JS19b1 [46] and *A. aromaticum* EbN1 [28]. Co-expression of other aromatic-degrading proteins (involved in *p*-cresol and phenol) on benzoate has been shown previously [41,45] for *G. metallireducens*. However, co-expression of benzoate-degrading and butyrate-degrading pathways during growth on butyrate has not yet been reported. Therefore, not only reported aromatic inducers, such as benzoate, phenol, and *p*-cresol [26], but also the fatty acid butyrate can activate the transcriptional regulators of benzoate degradation.

Central pathways and their regulation

In *G. metallireducens*, the TCA cycle is an important pathway through which 90% of carbon flux is channeled [49]. During acetate amendment in the field, high fluxes through the TCA cycle were found to correspond to high abundances of the TCA cycle proteins [17]. Similarly, in our study, highly abundant enzymes of the TCA cycle were also found. However, in contrast to Fang et al. [17], it was not possible to identify high abundances of citrate synthase (Gmet_1124) and succinyl:acetate coenzyme A transferase (Gmet_1125) under all conditions tested. According to our results (Supplementary Table S4), it appeared that in batch culture *G. metallireducens* primarily involves these enzymes in butyrate consumption, whereas in the environment, all homologues citrate synthases (Gmet_1124 and Gmet_2689) and succinyl:acetate coenzyme A transferases (Gmet_1125 and Gmet_3044) are activated during acetate amendment [17].

G. metallireducens was predicted to contain futile cycles of ATP consumption in its central metabolism [48]. Based on microarray data of *G. metallireducens* cultivated in acetate and benzoate-limited chemostats [9], Sun et al. concluded that *G. metallireducens* up-regulates energy-inefficient ATP-consuming reactions during growth on carbon sources, such as benzoate [48]. In the current study, only acetyl-CoA hydrolase (Gmet_2054) (later annotated as succinyl:benzoate coenzyme A transferase [40]) was found to be significantly expressed on benzoate. However, according to Oberender et al. [40], the latter enzyme is associated with benzoate activation rather than with participation in futile cycles. Therefore, in contrast to carbon limitation in chemostats, *G. metallireducens* does not restrict its growth via energy-inefficient reactions on complex substrates, such as benzoate or toluene, during exponential growth in batch culture. Obviously, such a strategy is important for providing fast growth rates and high biomass yields.

As expected, the activating reactions of toluene, ethanol, and butyrate degradation are regulated by changes in the corresponding enzyme levels. In contrast, changes in the flux through the enzymes of central metabolism (the TCA cycle), in response to growth on different substrates, are primarily regulated by changes in metabolite concentrations, rather than by changes in gene expression. The advantages of metabolic regulation of the TCA cycle for *G. metallireducens* are a reduction in energetic costs, as protein synthesis is ATP demanding [47], and the provision of plasticity in the physiological response to environmental changes.

In conclusion, the current study revealed that under high substrate concentrations *G. metallireducens* preferred utilization of the easily degradable substrates acetate and ethanol over benzoate. However, at the protein expression level acetate did not lead to strong repression of the expression level of the benzoyl-CoA pathway. Moreover, the short chain fatty acid butyrate might be involved in the activation of the benzoyl-CoA pathway and prepare microorganisms for degrading aromatic compounds in polluted environments. Therefore, it is concluded that *G. metallireducens* is well-adapted to habitats rich in aromatic compounds and fermentation products, such as fatty acids and ethanol.

Acknowledgements

This work was supported by the EU initial training network (ITN) project “Goodwater” (Grant Agreement Number 212683). We thank Kathleen Eismann and Christine Schumann for excellent technical assistance, and Dr. Housna Mouttaki for her valuable comments. Jana Seifert and Martin von Bergen were partially supported by DFG SPP1319.

Appendix A. Supplementary data

Supplementary data associated with this article can be found, in the online version, at http://dx.doi.org/10.1016/j.syapm.2014.02.004.

References

[1] Aklujkar, M., Krushkal, J., DiBartolo, G., Lapidus, A., Land, M.L., Lovley, D.R. (2009) The genome sequence of *Geobacter metallireducens*: features of metabolism, physiology and regulation common and dissimilar to *Geobacter sulfurreducens*. BMC Microbiol. 9, 109.

[2] Aklujkar, M., Haveman, S.A., DiDonato, R., Jr., Chertkov, O., Han, C.S., Land, M.L., Brown, P., Lovley, D.R. (2012) The genome of *Pelobacter carbinolicus* reveals surprising metabolic capabilities and physiological features. BMC Genomics 13, 8.

[3] Alexa, A., Rahnenfuehrer, J., Lengauer, T. (2006) Improved scoring of functional groups from gene expression data by decorrelating GO graph structure. Bioinformatics 22, 1600–1607.

[4] Anneser, B., Einsiedl, F., Meckenstock, R.U., Richters, L., Wisotzky, F., Griebler, C. (2008) High-resolution monitoring of biogeochemical gradients in a tar oil-contaminated aquifer. Appl. Geochem. 23, 1715–1730.

[5] Barragan, M.J.L., Carmona, M., Zamarro, M.T., Thiele, B., Boll, M., Fuchs, G., Garcia, J.L., Diaz, E. (2004) The *bzd* gene cluster, coding for anaerobic benzoate catabolism, in *Azoarcus* sp. strain CIB. J. Bacteriol. 186, 5762–5774.

[6] Bastida, F., Rosell, M., Franchini, A.G., Seifert, J., Finsterbusch, S., Jehmlich, N., Jechalke, S., von Bergen, M., Richnow, H.H. (2010) Elucidating MTBE degradation in a mixed consortium using a multidisciplinary approach. FEMS Microbiol. Ecol. 73, 370–384.

[7] Bradford, M.M. (1976) A rapid and sensitive method for the quantitation of microgram quantities of protein utilizing the principle of protein-dye binding. Anal. Biochem. 72, 248–254.

[8] Braunschweig, J., Bosch, J., Heister, K., Kuebeck, C., Meckenstock, R.U. (2012) Reevaluation of colorimetric iron determination methods commonly used in geomicrobiology. J. Microbiol. Methods 89, 41–48.

[9] Butler, J.E., He, Q., Nevin, K.P., He, Z.L., Zhou, J.Z., Lovley, D.R. (2007) Genomic and microarray analysis of aromatics degradation in *Geobacter metallireducens* and comparison to a *Geobacter* isolate from a contaminated field site. BMC Genomics 8, 180.

[10] Christensen, T.H., Bjerg, P.L., Banwart, S.A., Jakobsen, R., Heron, G., Albrechtsen, H.J. (2000) Characterization of redox conditions in groundwater contaminant plumes. J. Contam. Hydrol. 45, 165–241.

[11] Cox, J., Mann, M. (2008) MaxQuant enables high peptide identification rates, individualized p.p.b.-range mass accuracies and proteome-wide protein quantification. Nat. Biotechnol. 26, 1367–1372.

[12] Cox, J., Neuhauser, N., Michalski, A., Scheltema, R.A., Olsen, J.V., Mann, M. (2011) Andromeda: a peptide search engine integrated into the MaxQuant environment. J. Proteome Res. 10, 1794–1805.

[13] Da Silva, M.L.B., Ruiz-Aguilar, G.M.L., Alvarez, P.J.J. (2005) Enhanced anaerobic biodegradation of BTEX-ethanol mixtures in aquifer columns amended with sulfate, chelated ferric iron or nitrate. Biodegradation 16, 105–114.

[14] Dennis, G., Sherman, B.T., Hosack, D.A., Yang, J., Gao, W., Lane, H.C., Lempicki, R.A. (2003) DAVID: database for annotation, visualization, and integrated discovery. Genome Biol. 4, 1–11.

[15] Ding, Y.-H.R., Hixson, K.K., Giometti, C.S., Stanley, A., Esteve-Nunez, A., Khare, T., Tollaksen, S.L., Zhu, W., Adkins, J.N., Lipton, M.S., Smith, R.D., Mester, T., Lovley, D.R. (2006) The proteome of dissimilatory metal-reducing microorganism *Geobacter sulfurreducens* under various growth conditions. Biochim. Biophys. Acta 1764, 1198–1206.

[16] Falcon, S., Gentleman, R. (2007) Using GOstats to test gene lists for GO term association. Bioinformatics 23, 257–258.

[17] Fang, Y., Wilkins, M.J., Yabusaki, S.B., Lipton, M.S., Long, P.E. (2012) Evaluation of a genome-scale *in silico* metabolic model for *Geobacter metallireducens* by using proteomic data from a field biostimulation experiment. Appl. Environ. Microbiol. 78, 8735–8742.

[18] Foght, J. (2008) Anaerobic biodegradation of aromatic hydrocarbons: pathways and prospects. J. Mol. Microbiol. Biotechnol. 15, 93–120.

[19] Gorke, B., Stulke, J. (2008) Carbon catabolite repression in bacteria: many ways to make the most out of nutrients. Nat. Rev. Microbiol. 6, 613–624.

[20] Grimmler, C., Held, C., Liebl, W., Ehrenreich, A. (2010) Transcriptional analysis of catabolite repression in *Clostridium acetobutylicum* growing on mixtures of D-glucose and D-xylose. J. Bacteriol. 150, 315–323.

[21] Hallbeck, L., Pedersen, K. (2008) Characterization of microbial processes in deep aquifers of the Fennoscandian shield. Appl. Geochem. 23, 1796–1819.

[22] Hammer, Ø., Harper, D.A.T., Ryan, P.D. (2001) PAST: paleontological statistics software package for education and data analysis. Palaeontol. Electron. 4 (1), 9.

[23] Heintz, D., Gallien, S., Wischgoll, S., Ullmann, A.K., Schaeffer, C., Kretzschmar, A.K., van Dorsselaer, A., Boll, M. (2009) Differential membrane proteome analysis reveals novel proteins involved in the degradation of aromatic compounds in *Geobacter metallireducens*. Mol. Cell Proteomics 8, 2159–2169.

[24] http://www-stat.stanford.edu/tibs/SAM/sam.pdf.

[25] Jehmlich, N., Schmidt, F., Hartwich, M., von Bergen, M., Richnow, H.-H., Vogt, C. (2008) Incorporation of carbon and nitrogen atoms into proteins measured by protein-based stable isotope probing (Protein-SIP). Rapid Commun. Mass Spectrom. 22, 2889–2897.

[26] Juárez, J.F., Zamarro, M.T., Barragan, M.J.L., Blázquez, B., Boll, M., Kuntze, K., García, J.L., Díaz, E., Carmona, M. (2010) Identification of the *Geobacter metallireducens* BamVW two-component system, involved in transcriptional regulation of aromatic degradation. Appl. Environ. Microbiol. 76, 383–385.

[27] Kube, M., Heider, J., Amann, J., Hufnagel, P., Kühner, S., Beck, A., Reinhardt, R., Rabus, R. (2004) Genes involved in the anaerobic degradation of toluene in a denitrifying bacterium, strain EbN1. Arch. Microbiol. 181, 182–194.

[28] Kühner, S., Wohlbrand, L., Fritz, I., Wruck, W., Hultschig, C., Hufnagel, P., Kube, M., Reinhardt, R., Rabus, R. (2005) Substrate-dependent regulation of anaerobic degradation pathways for toluene and ethylbenzene in a denitrifying bacterium, strain EbN1. J. Bacteriol. 187, 1493–1503.

[29] Laemmli, U.K. (1970) Cleavage of structural proteins during the assembly of the head of bacteriophage T4. Nature 227, 680–685.

[30] Li, D.H., Yan, Y.L., Ping, S.Z., Chen, M., Zhang, W., Li, L., Lin, W.N., Geng, L.Z., Liu, W., Lu, W., Lin, M. (2010) Genome-wide investigation and functional characterization of the beta-ketoadipate pathway in the nitrogen-fixing and root-associated bacterium *Pseudomonas stutzeri* A1501. BMC Microbiol. 10, 36.

[31] Lovley, D.R., Phillips, E.J. (1988) Novel mode of microbial energy metabolism: organic carbon oxidation coupled to dissimilatory reduction of iron or manganese. Appl. Environ. Microbiol. 54, 1472–1480.

[32] Lovley, D.R., Giovannoni, S.J., White, D.C., Champine, J.E., Phillips, E.J., Gorby, Y.A., Goodwin, S. (1993) *Geobacter metallireducens* gen. nov. sp. nov., a microorganism capable of coupling the complete oxidation of organic compounds to the reduction of iron and other metals. Arch. Microbiol. 159, 336–344.

[33] Lovley, D.R., Ueki, T., Zhang, T., Malvankar, N.S., Shrestha, P.M., Flanagan, K.A., Aklujkar, M., Butler, J.E., Giloteaux, L., Rotaru, A.-E., Holmes, D.E., Franks, A.E., Orellana, R., Risso, C., Nevin, K.P. (2011) Geobacter: the microbe electric's physiology, ecology, and practical applications. In: Poole, R.K. (Ed.),. Adv. Microb. Physiol., 1–100.

[34] Marozava, S., Röling, W.F.M., Seifert, J., Köffner, R., von Bergen, M., Meckenstock, R.U. (2014) Physiology of *Geobacter metallireducens* under excess and limitation of electron donors. Part II. Mimicking environmental conditions during cultivation in retentostats. Syst. Appl. Microbiol (accepted for publication).

[35] Mazzoli, R., Pessione, E., Giuffrida, M.G., Fattori, P., Barello, C., Giunta, C., Lindley, N.D. (2007) Degradation of aromatic compounds by *Acinetobacter radioresistens* S13: growth characteristics on single substrates and mixtures. Arch. Microbiol. 188, 55–68.

[36] McMahon, P.B., Vroblesky, D.A., Bradley, P.M., Chapelle, F.H., Gullett, C.D. (1995) Evidence for enhanced mineral dissolution in organic acid-rich shallow ground water. Ground Water 33, 207–216.

[37] Monod, J. 1942 Recherches sur la croissance des cultures bacteíriennes, Hermann et Cie, Paris, France.

[38] Morales, G., Linares, J.F., Beloso, A., Albar, J.P., Martinez, J.L., Rojo, F. (2004) The *Pseudomonas putida* Crc global regulator controls the expression of genes from several chromosomal catabolic pathways for aromatic compounds. J. Bacteriol. 186, 1337–1344.

[39] Nguyen, T.N., Borges, K.M., Romano, A.H., Noll, K.M. (2001) Differential gene expression in *Thermotoga neapolitana* in response to growth substrate. FEMS Microbiol. Lett. 195, 79–83.

[40] Oberender, J., Kung, J.W., Seifert, J., von Bergen, M., Boll, M. (2012) Identification and characterization of a succinyl-coenzyme A (CoA):benzoate CoA transferase in *Geobacter metallireducens*. J. Bacteriol. 194, 2501–2508.

[41] Peters, F., Heintz, D., Johannes, J., van Dorsselaer, A., Boll, M. (2007) Genes, enzymes, and regulation of para-cresol metabolism in *Geobacter metallireducens*. J. Bacteriol. 189, 4729–4738.

[42] Rocha, E.P.C. (2008) The organization of the bacterial genome. Annu. Rev. Genet. 42, 211–233.

[43] Rossell, S., van der Weijden, C.C., Kruckeberg, A.L., Bakker, B.M., Westerhoff, H.V. (2005) Hierarchical and metabolic regulation of glucose influx in starved *Saccharomyces cerevisiae*. FEMS Yeast Res. 5, 611–619.

[44] Ruiz-Aguilar, G.M.L., Fernandez-Sanchez, J.M., Kane, S.R., Kim, D., Alvarez, P.J.J. (2002) Effect of ethanol and methyl-tert-butyl ether on monoaromatic hydrocarbon biodegradation: Response variability for different aquifer materials under various electron-accepting conditions. Environ. Toxicol. Chem. 21, 2631–2639.

[45] Schleinitz, K.M., Schmeling, S., Jehmlich, N., von Bergen, M., Harms, H., Kleinsteuber, S., Vogt, C., Fuchs, G. (2009) Phenol degradation in the strictly anaerobic iron-reducing bacterium *Geobacter metallireducens* GS-15. Appl. Environ. Microbiol. 75, 3912–3919.

[46] Seo, J.S., Keum, Y.S., Li, Q.X. (2011) Comparative protein and metabolite profiling revealed a metabolic network in response to multiple environmental contaminants in *Mycobacterium aromativorans* JS19b1(T). J. Agric. Food Chem. 59, 2876–2882.

[47] Stouthamer, A.H. (1973) A theoretical study on the amount of ATP required for synthesis of microbial cell material. Antonie Van Leeuwenhoek 39, 545–565.

[48] Sun, J., Sayyar, B., Butler, J.E., Pharkya, P., Fahland, T.R., Famili, I., Schilling, C.H., Lovley, D.R., Mahadevan, R. (2009) Genome-scale constraint-based modeling of *Geobacter metallireducens*. BMC Syst. Biol. 3, 174.

[49] Tang, Y.J., Chakraborty, R., Martin, H.G., Chu, J., Hazen, T.C., Keasling, J.D. (2007) Flux analysis of central metabolic pathways in *Geobacter metallireducens* during reduction of soluble Fe(III)-nitrilotriacetic acid. Appl. Environ. Microbiol. 73, 3859–3864.

[50] ter Kuile, B.H., Westerhoff, H.V. (2001) Transcriptome meets metabolome: hierarchical and metabolic regulation of the glycolytic pathway. FEBS Lett. 500, 169–171.

[51] Trautwein, K., Grundmann, O., Woehlbrand, L., Eberlein, C., Boll, M., Rabus, R. (2011) Benzoate mediates repression of C(4)-dicarboxylate utilization in *Aromatoleum aromaticum* EbN1. J. Bacteriol. 194, 518–528.

[52] Tusher, V.G., Tibshirani, R., Chu, G. (2001) Significance analysis of microarrays applied to the ionizing radiation response. Proc. Natl. Acad. Sci. U. S. A. 98, 5116–5121.
[53] Ueki, T. (2011) Identification of a transcriptional repressor involved in benzoate metabolism in *Geobacter bemidjiensis*. Appl. Environ. Microbiol. 77, 7058–7062.
[54] Vargas, M., Noll, K.M. (1996) Catabolite repression in the hyperthermophilic bacterium *Thermotoga neapolitana* is independent of cAMP. Microbiology 142, 139–144.
[55] Vinuselvi, P., Kim, M.K., Lee, S.K., Ghim, C.-M. (2012) Rewiring carbon catabolite repression for microbial cell factory. BMP Rep. 45, 59–70.
[56] Wischgoll, S., Heintz, D., Peters, F., Erxleben, A., Sarnighausen, E., Reski, R., Van Dorsselaer, A., Boll, M. (2005) Gene clusters involved in anaerobic benzoate degradation of *Geobacter metallireducens*. Mol. Microbiol. 58, 1238–1252.
[57] Yu, C.L., Louie, T.M., Summers, R., Kale, Y., Gopishetty, S., Subramanian, M. (2009) Two distinct pathways for metabolism of theophylline and caffeine are coexpressed in *Pseudomonas putida* CBB5. J. Bacteriol. 191, 4624–4632.
[58] Yu, N.Y., Laird, M.R., Spencer, C., Brinkman, F.S.L. (2011) PSORTdb-an expanded, auto-updated, user-friendly protein subcellular localization database for Bacteria and Archaea. Nucleic Acids Res. 39, D241–D244.
[59] Zimmermann, T., Sorg, T., Siehler, S.Y., Gerischer, U. (2009) Role of *Acinetobacter baylyi* Crc in catabolite repression of enzymes for aromatic compound catabolism. J. Bacteriol. 191.